PSFC/RR-97-4

Feasibility of the TPX fiber optic temperature-sensor quench detection system

Joel Schultz and Steve Smith

March 5, 1997

Plasma Science and Fusion Center
Massachusetts Institute of Technology
Cambridge, MA 02139 USA

This work was supported by the U.S. Department of Energy Contract No. DE-AC02-76-CH03073. Reproduction, translation, publication, use and disposal, in whole or in part by or for the United States government is permitted.

Feasibility of the TPX fiber optic temperature-sensor quench detection system

Joel Schultz and Steve Smith

M.I.T. PFC Report/ PSFC/RR-97-4

March 5, 1997

ABSTRACT

The Tokamak Physics Experiment (TPX) was a steady-state, tokamak to be built at the Princeton Plasma Physics Laboratory. It would have been the first tokamak in the world with an entirely superconducting magnet system. The project was terminated by the United States Congress in 1995. However, most of the TPX mission has been adopted recently by the South Korean project KSTAR (Korean Superconducting Tokamak Advanced Reactor) experiment at the Korean Basic Science Institue (KBSI). The principal obstacle to an all-superconducting tokamak magnet system has been the difficulty in detecting a quench and protecting the coil system in a high-noise, high-voltage environment. TPX adopted a a redundant, high noise-rejection design that will also be applicable to KSTAR.

The purpose of this memorandum is to summarize the information that leads us to conclude that a fiber-optic temperature sensor system alone should be adequate to protect the Tokamak Physics Experiment (TPX) magnets, in the event of a quench. Because of the importance of coil protection, the quench detection design philosophy for TPX is to require independent quench detection systems, any one of which should be adequate. This memorandum reviews the design requirements, the design, analysis that shows compliance with the requirements, and test data that supports the analysis models.

I. Fiber Optic Sensor System Description

Fiberoptic sensors, internal to the cable-in-conduit superconductor (CICC), will detect quenches by measuring the temperature rise associated with a quench inside the superconducting cable. Fiberoptics have a number of advantages in this application including very high EMF immunity, insensitivity to high magnetic field, and insensitivity to high rate of change magnetic fields. They also have the unique advantage of being able to measure the temperature, the single most important thermodynamic variable describing the internal state of the CICC, noninvasively. This allows a higher degree of calibration of code predicting losses from nuclear radiation, superconductor pulsed losses, and 3D eddy currents. The fibers are also good insulators permitting easy non-electric extraction, and very low loss, allowing long, continuous sensing lengths.

An inventory of fiber optic sensors within the coil winding packs is given in Table I. In the absence of an SDD, the PF lengths are taken from a global analysis by Pillsbury[1].

Table I: Inventory of Fiber Optic Sensors

Coil	Ncoils	$L_{winding\ pack}$	Fibers/cable	$L_{FO\ tubes}$	$L_{optical\ fiber}$
		(km)		(km)	(km)
TF	16	1.1	17	18.7	37.4
PF1	2	0.61	2	1.22	2.44
PF2	2	0.49	2	0.98	1.96
PF3	2	0.31	2	0.62	1.24
PF4	2	0.31	2	0.62	1.24
PF5	2	0.98	2	1.96	3.92
PF6	2	2.83	2	5.66	11.32
PF7	2	2.27	2	4.54	9.08
Total	30			34.3	68.6

I.A Fiberoptics Basics

The fiberoptics used here are very similar to conventional single-mode communications fibers, shown schematically in Fig. 1. The fiber consists of a lightly doped, very pure silica core about 5 microns in diameter (depending on the operating wavelength) surrounded by a very pure silica cladding layer about 125 microns in diameter. The doping of the core causes the index of refraction of the core to be about 1 part in 1000 higher than the surrounding cladding. This index difference, in a very simple model for the waveguide, causes the light to be "trapped" in the core by total internal reflection at the core-cladding interface, as shown on the right of Fig. 1. Due to the very small index step and size on the fiber core, only one mode of the waveguide can propagate. This situation is very analogous to a simple particle in a box problem from quantum mechanics. In this case, the box is very shallow and narrow so there is only one bound solution.

[1] TPX No:14-941130-MIT-RPillsbury-01, R. D. Pillsbury, Jr. and J. H. Schultz, "Impact of the HC Scenario for TPX on the PF Magnets and Power Supplies," November 30, 1994

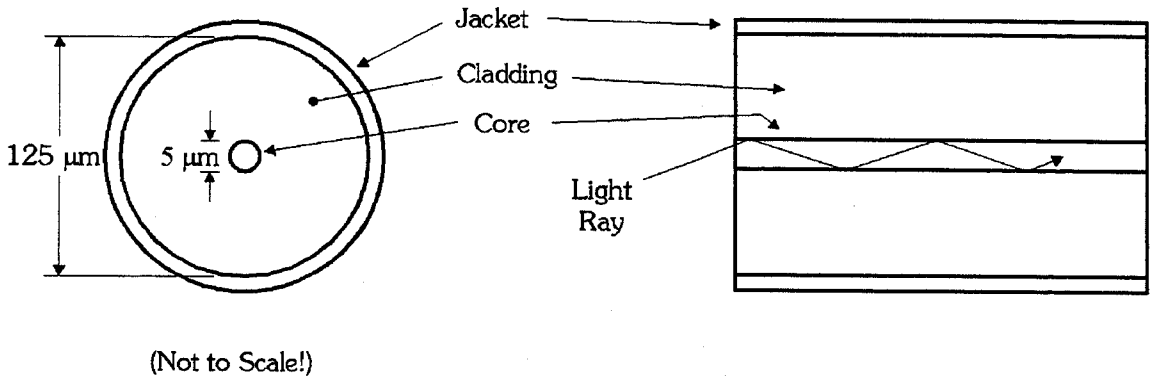

Figure 1 Schematic diagram of commercial single mode fiberoptic

Conventional communications are coated with a polymer to protect the fiber from damage. While fiberoptics are typically proof tested at 50 kpsi,[2] the strength of the fiber is dramatically degraded with even micron size scratches to the outside of the fiber. This effect is used to cut the ends of fiberoptics, where the fiber is held in a small jig and scratched using a ceramic or carbide bit, similar to scoring a piece of glass. The fiber is then broken by gently bending it, again very similar to the procedure used to cut larger pieces of glass. In a Nb_3Sn superconducting cable, the heat treatment procedure would destroy the polymer coating on the fiberoptics and leave the fiber very prone to damage. To avoid this, the polymer coating is replaced with a metallic coating on the fibers. Several metal coating fibers are commercially available including copper, gold, and aluminum. Copper and gold are compatible with the Nb_3Sn heat treatment. A diamond-like carbon coated fiber is also available. In the QUELL sample[3], a copper coated fiberoptic was used and has successfully been tested after cabling, insertion into the conduit, winding, and the initial heating phase of the heat treatment. The same copper coated fiberoptic would be used for the TPX fibers.

LB Sensor Physical Layout

Physically, the fiberoptic sensor is very similar to the internal voltage taps. In this case, two optical fibers are covered with an S-glass braid and encased in a stainless steel capillary tube (Fig. 2). This tube is then placed in the center of the final cabling stage, and will be located in the center of the final cable, as shown in Fig. 3.

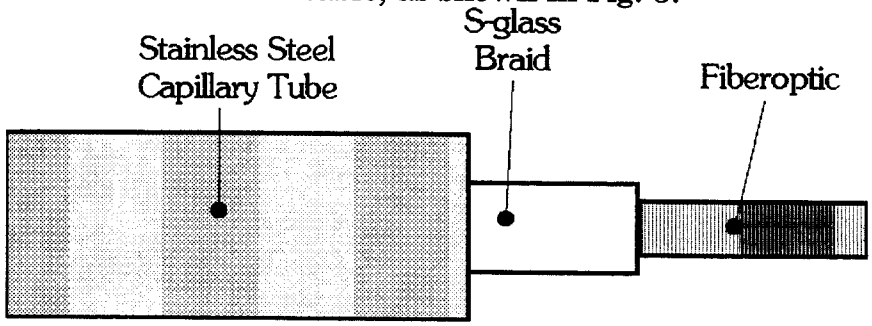

Figure 2 Internal fiberoptic sensor layout

[2]Fiber testing specs ref, 3M, or Corning.

[3] S. Pourrahimi, S. Smith et al, "US contributions to the development and calibration of quench detectors for the ITER QUELL," IEEE Trans Applied Superconductivity, Vol. 5, No. 2, June 1995

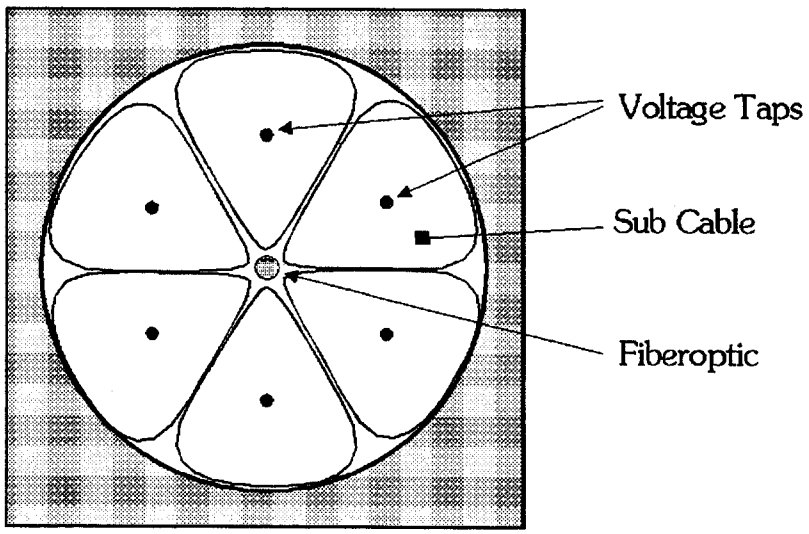

Figure 3 Internal sensor layout

Since the simple interferometric fiberoptic sensor measures the integrated temperature over its entire length, no information about the location of the quench is obtained.[4] In order to provide some information about the location of the quench, each of the fiberoptics is terminated once, inside the magnet, as shown in Fig. 4. At each of these terminations, the fiberoptic is cleaved and a metallic mirror is deposited on each of the two fiber faces. Thus, in the top fiber in the figure the light will enter the fiber at the left, travel 1/3 of the way through the magnet, be reflected by the metallic mirror, and then travel in the opposite direction through the same fiber and exit at the left. Similarly, light will also enter the top fiber from the right, travel 2/3 of the way through the cable, reverse direction at the mirror and emerge from the right side of the cable. Thus, these two fibers provide singly redundant temperature information about each 1/3 of the magnet.

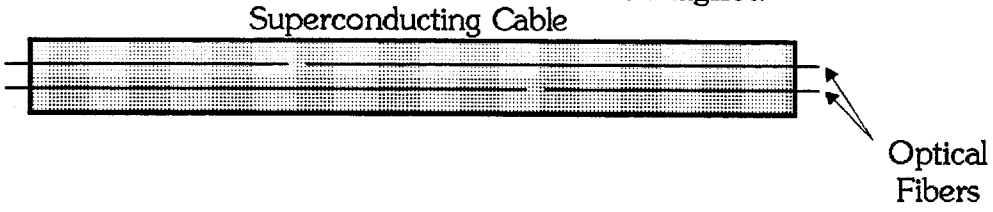

Figure 4 Internal termination positions for fiberoptic sensor

[4]There are other detection schemes using nonlinear effects in the optical fibers that have the ability to provide location information about the quench.

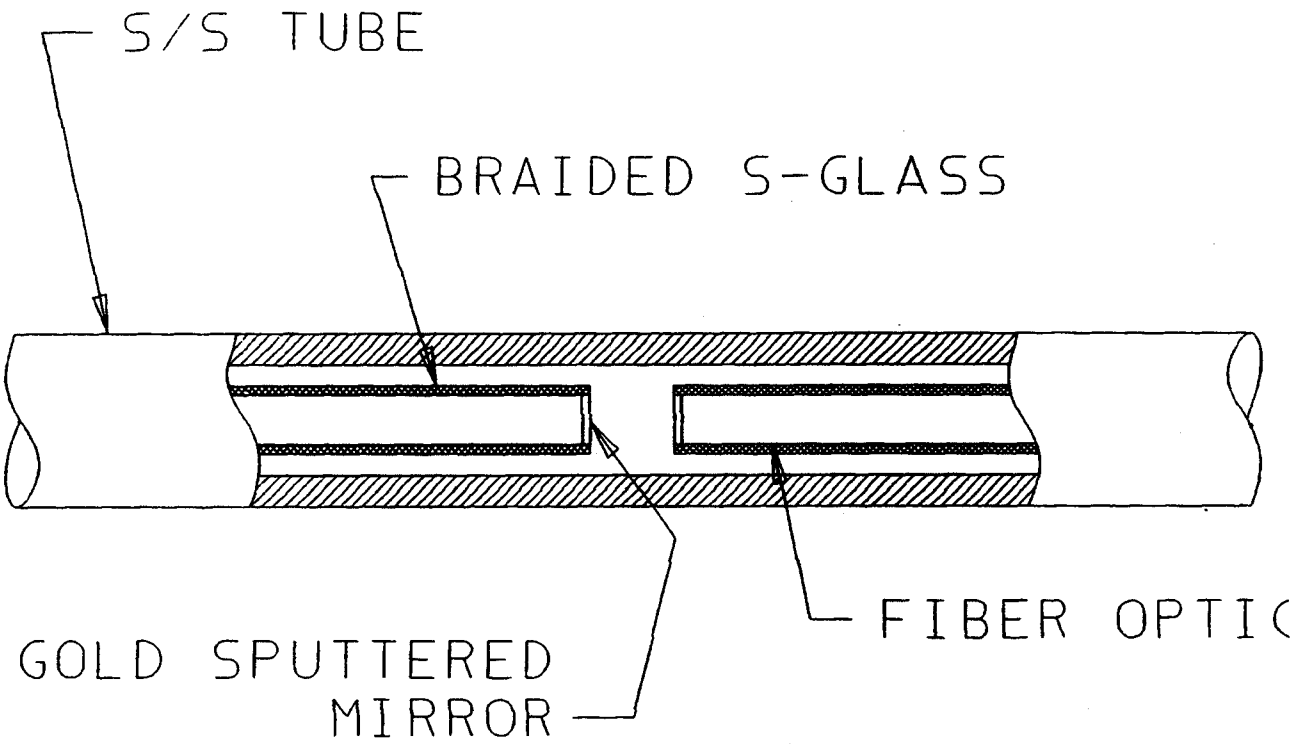

Figure 5 Fiber Optic Internal Termination Concept

LC Fiberoptic Instrumentation

The integrated temperature along each of the fiber segments is indirectly measured by interferometrically measuring the optical path length of each of the fiber segments. In this case, an all fiber Michelson interferometer is used, as shown in Fig. 5. As seen in the figure, light from a source is coupled into two fibers using the directional coupler labeled C in the figure. One of these arms, the sense arm, is inside the magnet being measured and the second arm, the reference arm, is held at a constant temperature. Light travels through each of these arms, is reflected by mirrors coated on the end of each of the fibers, and then returns through the same fiber. The light from each of these arms is then recombined, using the same directional coupler C, and then falls onto the detector labeled D in the figure. As the optical path length of the sensing arm changes, the light from the sensing and reference arms alternately constructively and destructively interferes, as shown in the right half of the figure. The optical path length change required to move from a point of constructive interference to another point of constructive interference, i.e., one fringe, is one half a wavelength of the light. By counting the number and direction of fringes, the change in optical path length of the sensing arm can be measured very accurately.

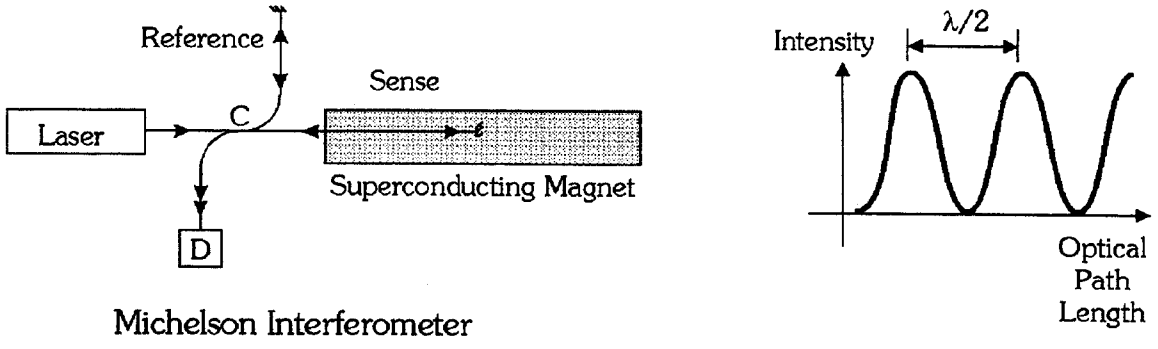

Figure 5 Michelson interferometer used with internal fiberoptic sensors

Since the fiberoptics are electrically insulating, all the fibers can be extracted through a single port in the cryostat wall. However, this may not be advantageous and multiple feedthroughs could also be used. It should also be noted that some components may be shared between interferometers. For example, in Fig. 6 several interferometers are shown sharing a common source, and, in Fig. 7, many of the discrete components are replaced with a very small, durable single integrated optic chip.

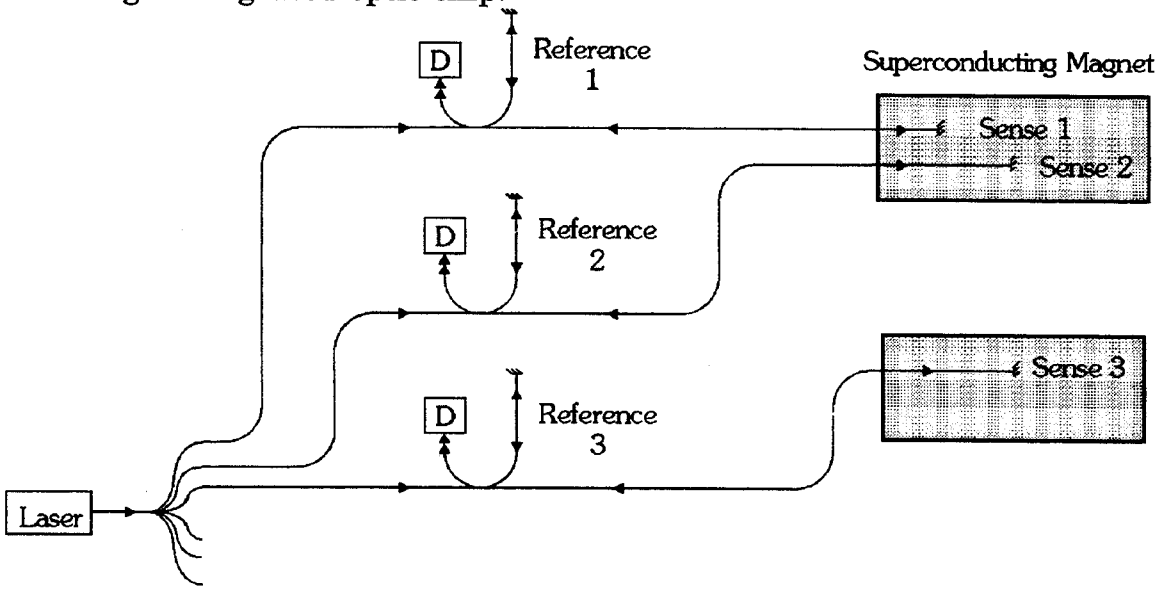

Figure 6 Several interferometers sharing a single source

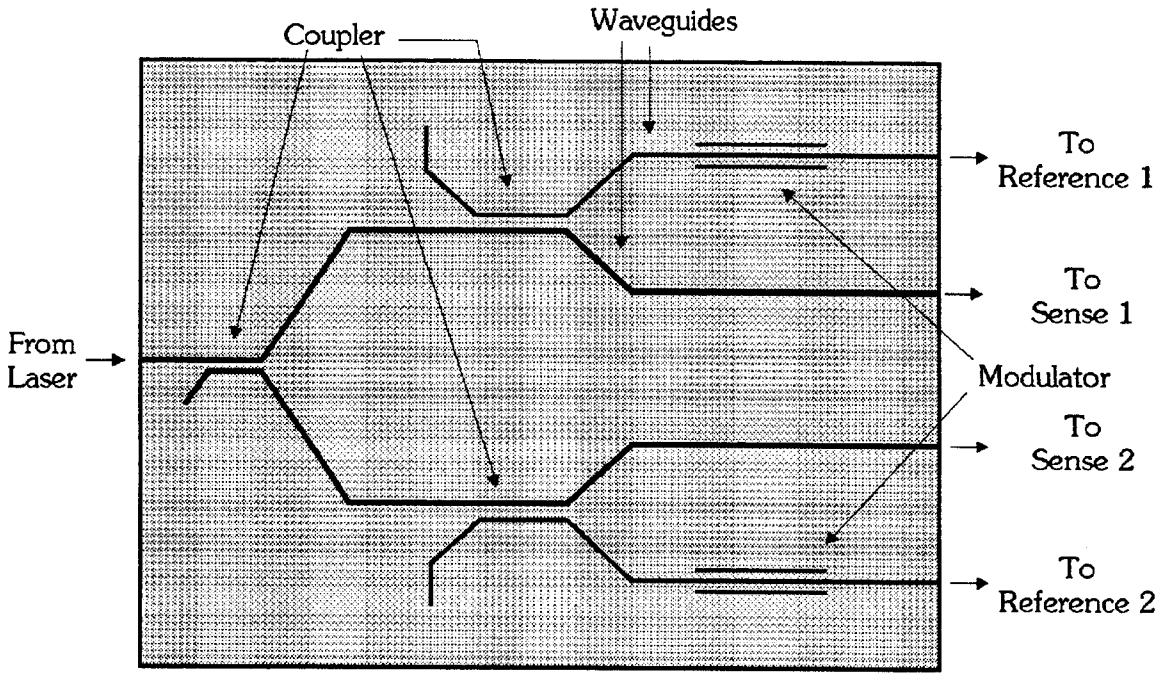

Integrated Optic Chip

Figure 7 A small durable integrated optic chip used to reduce the number of discrete optical components required for the fiberoptic sensors

II Sensor Mechanical Integrity

Internal voltage sensors should be capable of the following:

A) It should be possible to manufacture the sensor in one continuous length, at least equal to that of the longest cable in the magnet system. For the TPX design, this is 2.8 km in PF6. If a joint is added to PF6, it will be 1.4 km.

B) The sensor must be cabled or inserted in a cable along with the superconducting strands.

C) When the cable is inserted in a conduit and the cable is compacted about the cable and sensors, the sensors shouldn't be damaged.

D) The sensors must survive winding, along with the superconducting cable.

E) The sensors must survive heat treatment at temperatures up to 660 C.

F) The sensors must survive cooldown to 4 K.

G) Outgassing from the sensors shouldn't damage the superconductor or conduit. In particular, trapped oxygen or water shouldn't cause SAGBO in Incoloy 908.

H) The sensors must survive Lorentz loads.

II.A Length Limitations

Fiber optic sensors have no obvious length limitation. LaserArmorTech in San Diego routinely makes 50 km length of armored fiber optic lines. The seam-welded can about the fiber optic likewise has no obvious length limitations.

II.B&C Cabling, conduit insertion and compaction

Two types of fiber optic sensor were inserted into the QUELL conductor: one was copper-coated and the other had a conventional, commercial acrylic coating. This coating cannot survive the heat treatment, but protects the optical fiber during handling, especially cabling, prior to the heat treatment. During heat treatment, the coating "spatters" over the inside wall of the steel tube protecting the fiber, but the fiber remains intact. Although this technique has been demonstrated to work at the benchtop level at M.I.T., it was not definitively demonstrated in the QUELL coil, because Hitachi drilled through the tube and fiber (and possibly some nearby superconductors), when installing a pressure sensor. However, as of this morning (August 15, 1995), Shahin Pourrahimi reported from Switzerland that he had coupled laser light from one end to the other of the copper-coated fiber. This is the first demonstration of "beginning-to-end" feasibility of a fiber optic sensor in a medium-size, superconducting CICC.

II. D Winding

Copper and plastic-coated fibers were inserted into the QUELL dummy coil and into the QUELL superconducting coil by Hitachi. The coils were 120-133 m long. The inner turn winding radius was 25 cm, while the crossover minimum radius was about 20 cm. As mentioned immediately above, a copper-coated fiber has been shown to survive cabling, winding, heat treatment, and extraction in the superconducting QUELL coil.

Fiber-optic sensors were cowound in the MIT IGC 3.5:1 copper/noncopper ramp-rate limitation sample. Because the decision was made after the sample had already been cabled, they were external to the CICC conductor.

Fiber-optic sensors were cowound in the center of the MIT Superconducting Noise Injection Cable.

Fiber-optic sensors are being cowound in the center of the MIT 1 Rogowski/strand, TF Ramp-rate Limitation experiment.

II. E&F Heat treatment, sensor survival; survival of cooldown

Several tests have been done to investigate the survival of the optical fibers intended for the QUELL sample through the heat treatment and the cool down to liquid helium temperatures.

The most comprehensive test has been done on a length of copper coated optical fiber[5]. This fiber was inserted into a 1.0 mm stainless steel capillary tube, but with no S-glass braid, and subjected to a heat treatment of 700 C in a helium atmosphere for about 30 hours while wound in a 15 cm in diameter coil. This sample was then used as a

[5] TPX Memo 1314-941201-MIT/SSmith-01, S. Smith, "Fiber survival tests," Dec 1, 1994

demonstration piece and handled extensively at the Applied Superconductivity Conference in Boston, and allowed to sit in an uncontrolled atmosphere for several weeks. It was then rewound into a smaller diameter coil of ~ 8 cm, and immersed in a liquid helium bath. The sample survived all these procedures without any noticeable degradation. The 1.0 mm can surviving bending to an 8 cm radius and surviving a 700 C to 4 K temperature range, along with other handling, is more severe than the requirements for TPX, where the minimum bend radius for the conductor is 7.5 inches (19 cm).

Along with the heat treatment and winding test described immediately above, additional tests have also been performed on a number of other samples. Standard fiber samples have been baked up to 300 hours in an inert helium atmosphere at temperatures above 700 C without any measurable degradation in the optical characteristics of the fibers. Samples of specially coated diamond-like carbon and copper coated fibers have also been subjected to 100 hour heat treatments followed by immersion in liquid helium. Microscopic examination of these fibers revealed no visible damage to either type of jacketing material. Finally, both bare fibers and an s-glass covered fiber bundle have been inserted into stainless steel capillary tubes and heat treated for approximately 100 hours in a helium atmosphere. All the fibers in both of the samples survived.

II.F Heat treatment, compatibility with SAGBO

An experiment was done to show that the presence of glass in the sensor insulation wouldn't cause SAGBO. The experiment was designed to be orders of magnitude more severe than the actual design case. A 4" long section of Incoloy 908 tube, 19 mm o.d. and 17 mm i.d., was selected for the SAGBO cracking experiment. The Incoloy tube was from a stock that was produced by seam welding, and according to Mike Steeves this tube already had enough plastic strain for it to be prone to SAGBO cracking. However, in order to further strain the tube, the circular cross section of the tube was compressed to an oval cross section with major and minor dimensions of 21 and 15 mm respectively. Four 4" long pieces of a (Cu braid)-(s-glass)-Cu voltage sensor was placed inside the compressed tube. The assembly was then placed inside a quartz tube for evacuation and heat treatment. The quartz tube was evacuated to $3x10^{-5}$ torr. While still connected to the vacuum pump, the sample assembly was heat treated at 675 K for 4 hours and then at 795 K for 50 hours. After heat treatment the tube showed no visible signs of cracking. The heat treated tube was further compressed to a flatter oval of 8 mm minor dimension. Straining after heat treatment was more than 50% in the edges of the flattened tube and did not produce any cracking.

The real cable is chrome-coated and the partial pressure of oxygen above chrome from room temperature to 700 C is negigible. No oxygen getter was used inside the quartz tube, and no attempts, other than degreasing, were made to clean the tube before the heat treatment. The vacuum pump was one of the least powerful units in the laboratory and the pressure inside the quartz tube never reached values < 30^{-6} torrs. It should be pointed out that copper is itself a potential bad actor in terms of outgassing oxygen and that that the copper braid did not fully block outgassing from the S-glass.

II.G Lorentz loading

The peak Lorentz load on the tube carrying fibers would be IxB/A times a contact multiplication factor. The peak nominal load is 33.5 kA x 8.4 T/22.35 mm = 12.6 MPa. Ignoring contact stress multipliers, this is the equivalent of an external pressure of 12.6 MPa on a cylndrical vessel with a diameter of 1.0 mm and a thickness of 0.125 mm, giving a membrane stress of 50.4 MPa. This is less than a tenth of the yield strength of the steel can.

C. Radiation Resistance

A preliminary literature search by Smith[6] indicated that there were solutions that would give adequate radiation resistance for the case of ITER or DEMO and would certainly be adequate for the less severe radiation conditions of TPX.

The use of optical fibers in high radiation environments has been explored for a number of different applications.[7] While none of this readily available data exactly duplicates the conditions (operating temperature and radiation mixture) that the sensor fiber will experience in the TPX (or ITER) magnets, this data can at least be used as an indicator of the performance that can be expected.

The primary effect of the radiation on the optical fiber is to induce color centers in the core and cladding areas of the fiber, thus increasing the fiber loss. Figure 1 shows the induced fiber loss at 1.3 microns of a typical radiation hardened fiber as a function of total radiation dose for various dose rates.[8] It should be noted that if a 1 km length of fiber where exposed to the total expected radiation dose at the innner layer of a TPX magnet (10^7 rads or 10^5 Grays) over it's entire length (a pessimistic assumption) the induced loss would only be about 30 dB. Further, the induced attenuation in the fiber is frequency dependent and thus can be reduced by the appropriate choice of sensing laser wavelength. This level of loss in the sensor fiber could easily be accommodated.

Thus, preliminary indications are that the radiation induced attenuation should be at a manageable level. However, since the spectrum and strength of the radiation induced color centers has been shown to change with the temperature of the irradiated fibers,[9] tests will have to be done to closely mimic the expected environment of the fiber in the TPX coils.

---

[6] Stephen P. Smith, "Information on radiaiton effects on silica optical fibers," TPX 1314-950122-MIT/SSmith-01, January 22, 1995

[7] Judy K. Partin, "Fiber Optics in high dose radiation fields", SPIE vol. 541, Radiation Effects in Optical Materials, pg. 97-109 (1985).

[8] from Branko Leskovar, "OPTICAL DATA TRANSMISSION AT THE SUPERCONDUCTING SUPER COLLIDER", IEEE Transactions on Nuclear Science, vol. 37, No. 2, pg. 271-280 (1990).

[9] C. E. Barnes, "Irradiation and photobleaching of all-silica, pure silica core fibers at low temperatures", Proc. S.P.I.E. Int. Soc. Opt. Eng., vol. , pg. 47-54.

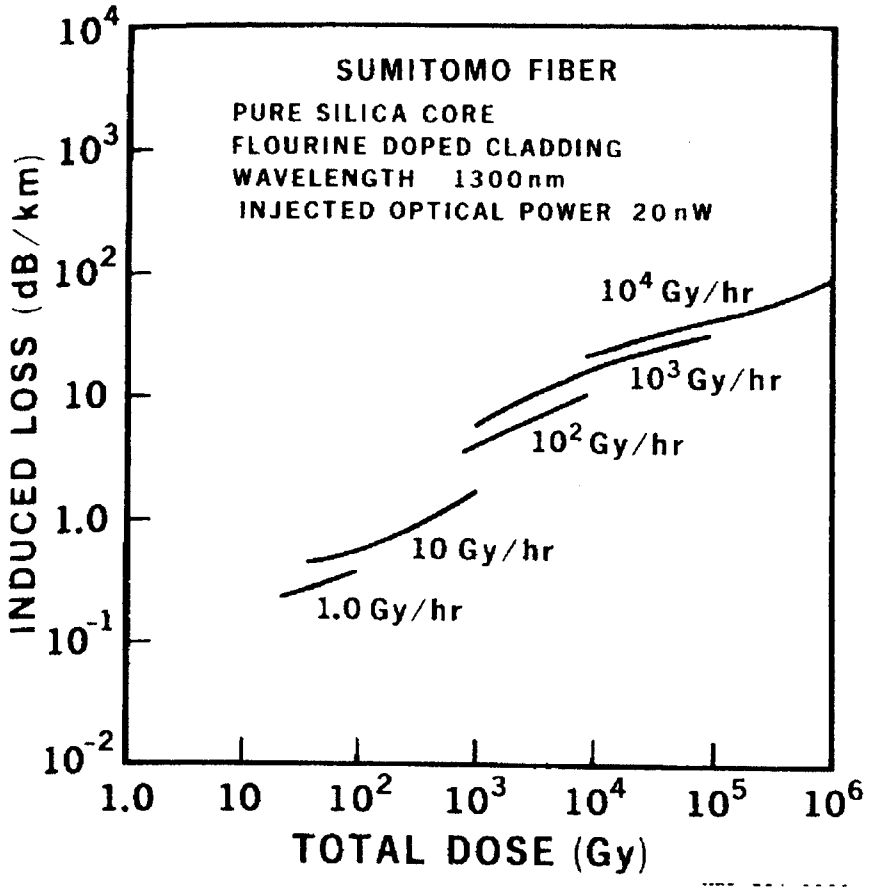

Figure 8 Induced attenuation in optical fibers as a function of the total radiation dose with dose rate as a parameter. The radiation source was Cobalt 60. (100 rad = 1 Gy)

In addition, some of the color centers responsible for this observed attenuation can be removed by optical bleaching. (They can also be removed by thermal annealing which obviously is not applicable here.) Barnes[10] sent a relatively strong optical beam through the fibers at 820 nm at 77 K and 195 K, in order to significantly reduce the strength of the radiation induced color centers, and hence the fiber loss. Laswer power of 60 and 90 μW was launched into a test fiber through a Y coupler. The results of the most relevant experiment are shown in Figure 9.

[10]C. E. Barnes, "Irradiation and photobleaching of all-silica, pure silica core fibers at low temperatures", Proc. S.P.I.E. Int. Soc. Opt. Eng., vol. , pg. 47-54.

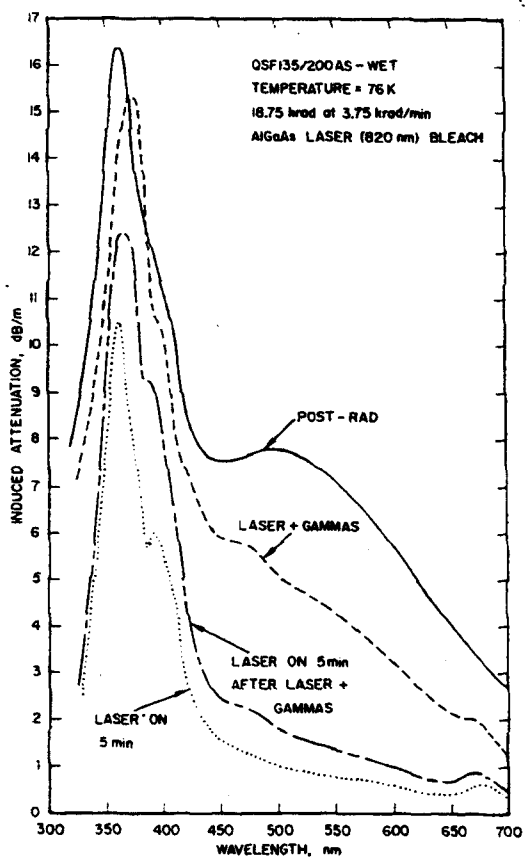

Figure 9: (Barnes, Proc. S.P.I.E.) A series of Co-60 induced attenuation spectra, following a sequence of irradiation and photobleaching steps at 76 K of a fluorosilicate clad, pure silica core fiber. The order of the sequence is 1) post rad, 2) laser on 5 min, 3) laser+gammas, and 4) laser on 5 min. after laser + gammas

The total irradiation of 18.75 krad used in this experiment is very small compared to the 109 rad expected in the highest-flux layers of a fusion TF magnet. However, the irradiation rate of 3.75 krad/min is high in comparison to that of a fusion magnet, which may accumulate its dose over a 10-20 year life. If we assume only a 10 year life and only 50 % availability, the rate would still be no higher than 0.38 krad/min. The highest attentuations would, of course, only be in the plasma-facing layers. Since the irradiation and bleaching times were equal at 5 minutes, this implies that photobleaching is a promising technique for real-time erasure of radiation-induced absorption and that further experiments should be done in more fusion-relevant conditions.

III. Signal-Noise Ratio

The sensitivity of a fiber-optic temperature sensor used for the purposes of calculating the signal-noise ratio is shown in Table II. The values here are interpolated from calibration measurements against a diode temperature sensor beginning at liquid helium

temperature[11]. The basic thermometry, calibrating the sesitivity of the interferometer vs. diode thermocouples, has also been done at room and liquid nitrogen temperature[12]. The signal-noise ratio of a quench vs. initiation or disruption is enhanced greatly by the sharp rise in sensitivity from liquid helium temperature to typical quench temperatures. The fiber sensitivity to temperature, based on experiments at M.I.T. with polymer jacketed fibers, is given by:

$$a = 3.5\,(T - 5);\ 5\,K < T < 9\,K \tag{1}$$

where a is the sensitivity of the fiber in Fringes/m-K and T is the temperature (K). Thus, the linearly increasing teperature produces a quadratically increasing fringe count (at least initially), according to the equation:

$$\int_5^T a\,dT = 1.75\,T^2 - 17.5\,T + 43.25;\ 5\,K < T < 9\,K \tag{2}$$

This increasing sensitivity saturates at about 15 fringes/m-K, and then only increases to about 25 fringes/m-K at room temperature. In order to calculate the signal/noise ratio of a quench vs. a disruption or initiation, the following table can be used:

Table II: Sensitivity of the fiber-optic temperature sensors

Temperature	Fringes/(K-m)	Fringes/m
5	0.	0
6	3.5	1.75
7	7	7
8	10.5	15.75
9	14	28
10	15	42.5
11	15.033	57.5165
12	15.067	72.5665
13	15.1	87.65
14	15.133	102.7665
15	15.167	117.9165
16	15.2	133.1
17	15.233	148.3165
18	15.267	163.5665
19	15.3	178.85
20	15.333	194.1665
21	15.367	209.5165
22	15.4	224.9
23	15.433	240.3165
24	15.467	255.7665
25	15.5	271.25
26	15.533	286.7665
27	15.567	302.3165
28	15.6	317.9
29	15.633	333.5165
30	15.667	349.1665

[11]ITER/US/94-EV-MAG/S.Smith/7.20/1, Stephen Smith and S. Ezekiel, "Fiberoptic Quench Detector: Liquid Helium Tests," July 20, 1994

[12] ITER No ITER/US/94/EV-MAG/S.Smith/6.21/-1, Stephen Smith and S. Ezekiel, "Optical Fiber Thermometry at Liquid Nitrogen Temperatures," June 9, 1994

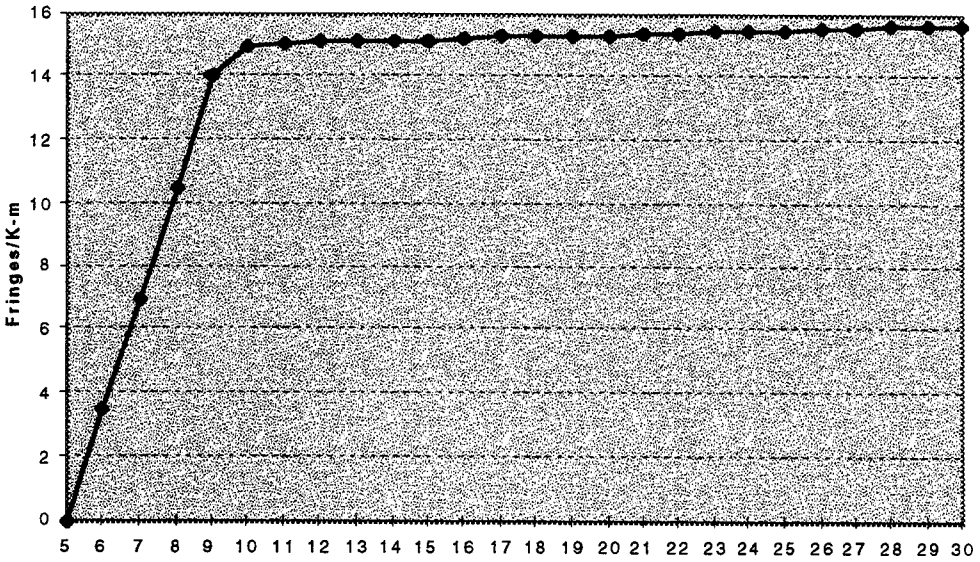

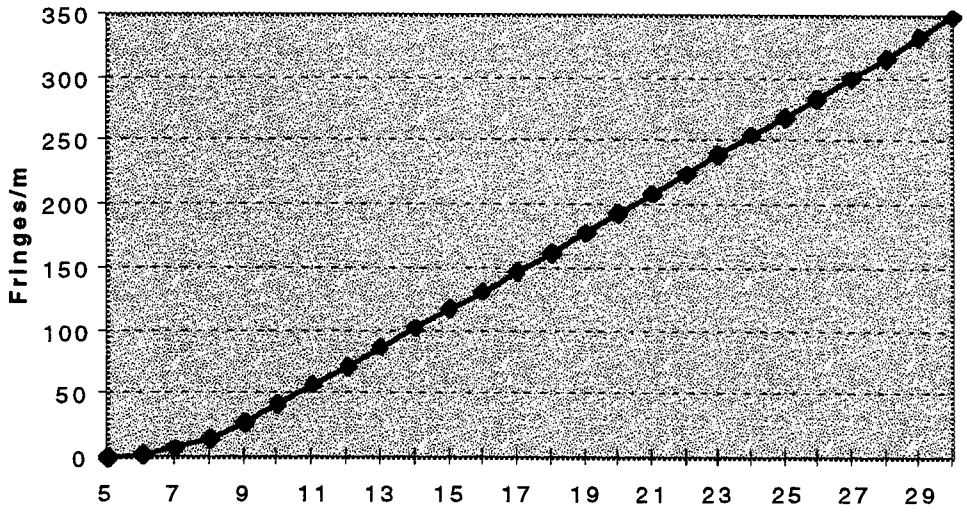

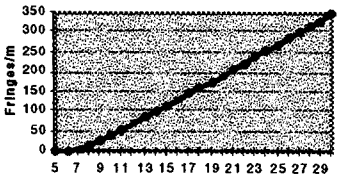

III.A Scenario/Disruption Signal

The fiber optic quench detector must be able to reject signals from normal scenarios and disruptions. A major concern has been that, since the fiber optic temperature sensor measures the integral of the temperature change over the entire length of the winding, while a quench may begin in a very short initial zone (~ 10 cm), the quench signal might get swamped by modest temperature rises over short distances. Simulations indicate that this is not the case, and that the signal/noise ratio of a fiber

optic QD system should be very high in a short period of time and that the system design criteria will be easily satisfied.

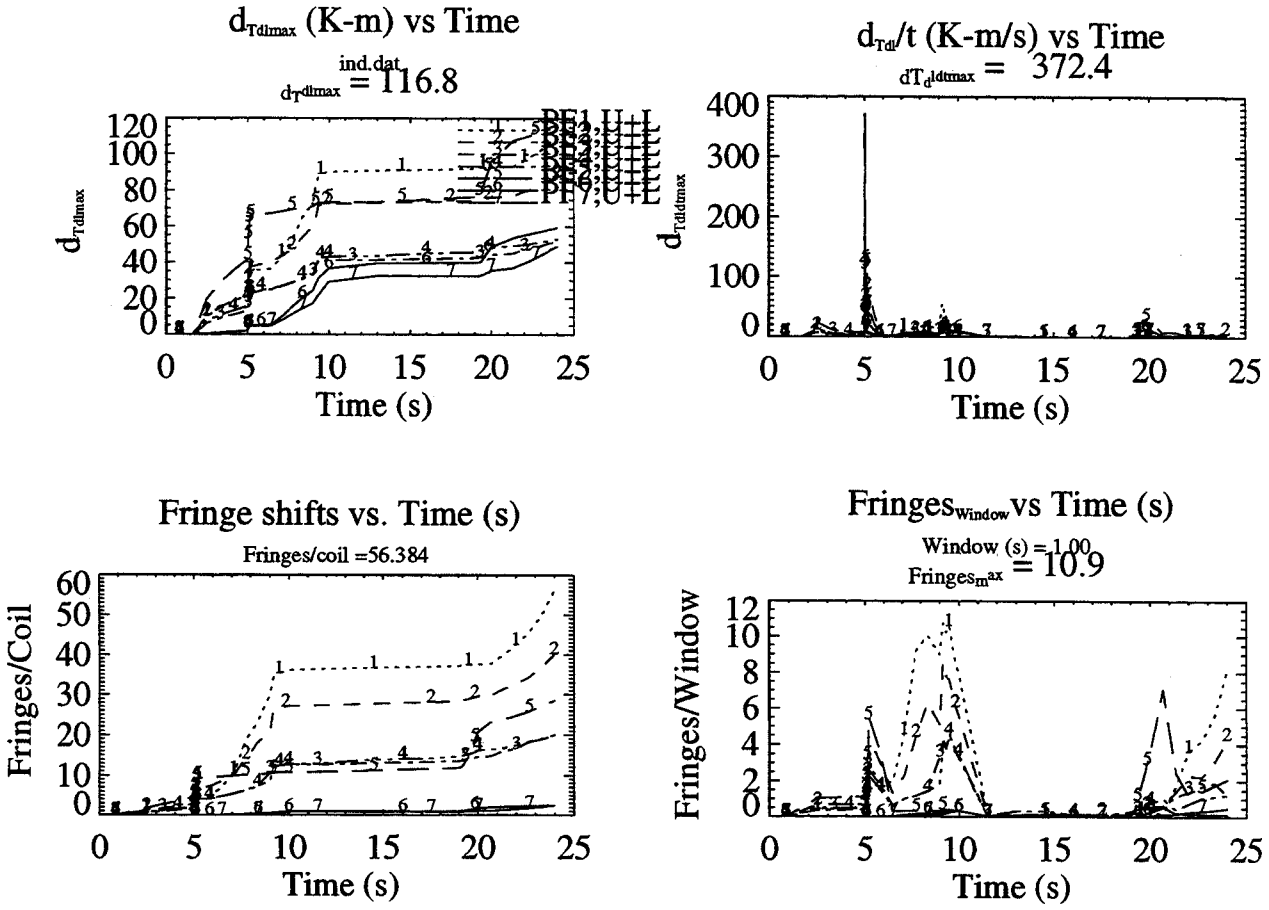

Figure 10: Temperature-length integral and interferometer fringe shifts in PF during normal HC Scenario

During an HC scenario, the worst PF coil in terms of temperature rise-length integral (m-K) is PF5 at 116.8 m-K, while the PF coil with the largest number of total fringe shifts/scenario is PF1 with 56.4. If we only look at the number of fringe shifts in the previous second, PF1 is still the worst with 11 fringes during heating to high beta. PF5 has 6 fringe shifts during plasma initiation and the first second of startup. If we recall that the fiber-optic temperature sensors divide the winding pack into 3 equal sections, the largest number of fringes in a second in a third of the PF1 winding pack would be ~ 2 fringe shifts. If assume that central difference averaging of the three sections reduces the differential signal by a factor of 10, the largest CDA signal from a normal HC scenario would be ~ 0.2 fringe shifts.

We now take the same HC scenario and terminate it with a vertical disruption at the End of Burn as shown in Figure 11. The disruption is coil-current-conserving, which gives an overly conservative estimation of total losses in the PF system.

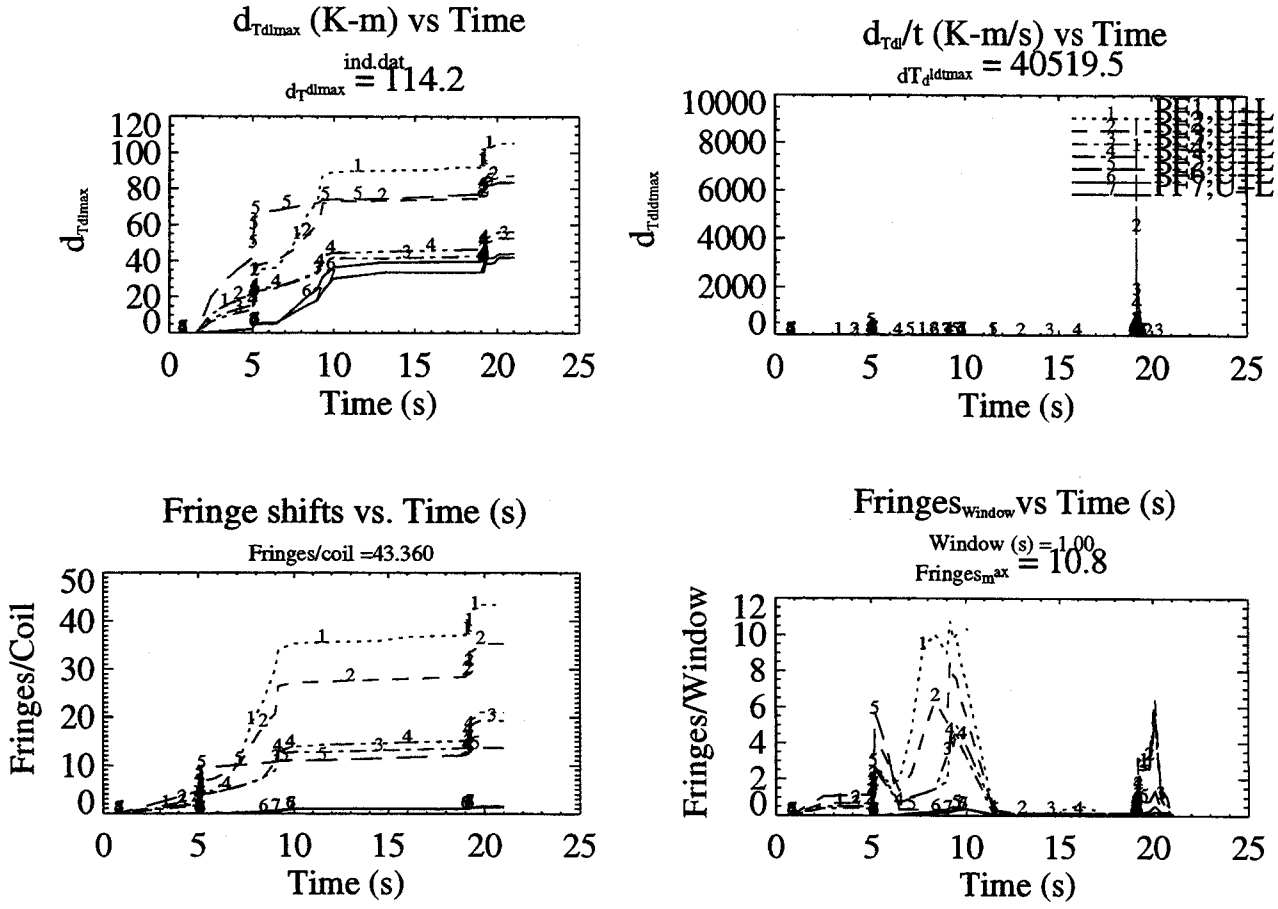

Figure 11: Fringe shifts in PF coils, due to an HC scenario, terminating in a plasma disruption

The total temperature-length integral and fringe shifts is slightly smaller than in the normal HC scenario. This is a little misleading, because the disruption scenario terminates with the disruption and doesn't include shutdown or quench/dump. If the scenario were completed, the disruption pulse would naturally have a higher temperature integral. However, the net result is that the disruption is no worse than the HC scenario in terms of its fringe shrift noise signal. Even though the instantaneous rate of fringe shifting is increased by a factor of over 100 from 372 m-K/s in the HC scenario to 40,520 m-K/s during the disruption, the integrated value of the disruption signal over a second is small. The maximum fringes in a second remains 10.9 in PF1 during heating to high beta. The maximum fringes during a disruption (and 1 second of eddy currents after the disruption) is 6.4 in PF1.

III.B Quench Signal

The quenches with the smallest Initial Quench Zones that have been simulated for the TF system are the 1 cm and 10 cm quenches, simulated by Shajii[13]. 10 cm quenches proved to give higher hot spot temperatures, as well as higher pressure and helium expulsion velocities, so 1 cm quenches, which are also numerically much harder to simulate, have been little studied. The only relevant data that can be extracted from Shajii's study is shown in Figure 12. This is the time evolution of a quench that began with a 1 cm IQZ at 1 second intervals. We assume that even if 1 cm is more benign than 10 cm for fixed detection time that it must be worse than 10 cm for detection based on a signal/noise ratio of 10:1. Eyeballing the temperature contour at 1 s, the integrated change in temperature-length is approximately 85 m-K. Even more crudely applying the fringe-sensitivities immediately above, the total number of fringe shifts are estimated to be 1300 in the first second of quench.

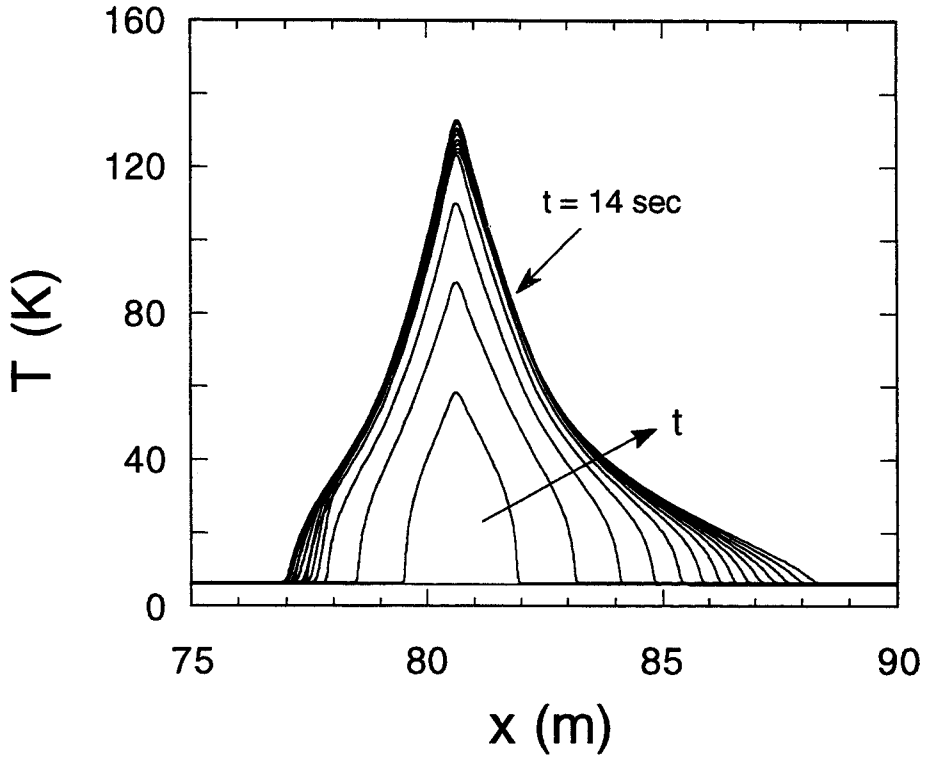

Fig 12: Conductor temperature profile at various time steps during quench

[13] TPX No. 13-941205-MIT-ASHAJII-01, A. Shajii, "Analysis of quench in the TPX TF coil with a "small" initial normal length," December 5, 1994

The PF quench voltages haven't been recalculated since the Technology Transfer Meeting of July 1994[14]. At the time, the short and long IQZ voltages were based on "hot-spot" dump scenarios that led to the peak temperatures, based on a large number of dump scenarios, simulated by Elaine Lu. Naturally, these would also give the highest and easiest to detect temperature signals. It is felt that this is always an unfavorable tradeoff and that harder to detect temperatures at lower currents will still lead to lower hot-spot temperatures when additional detection delays are taken into account. However, this assumption hasn't been quantitatively confirmed. The worst-case J2t was for 40,499 for PF5 at SOF, l_i=0.5, and β_N=2.2with 36,184 in the assumed second before quench initiation.

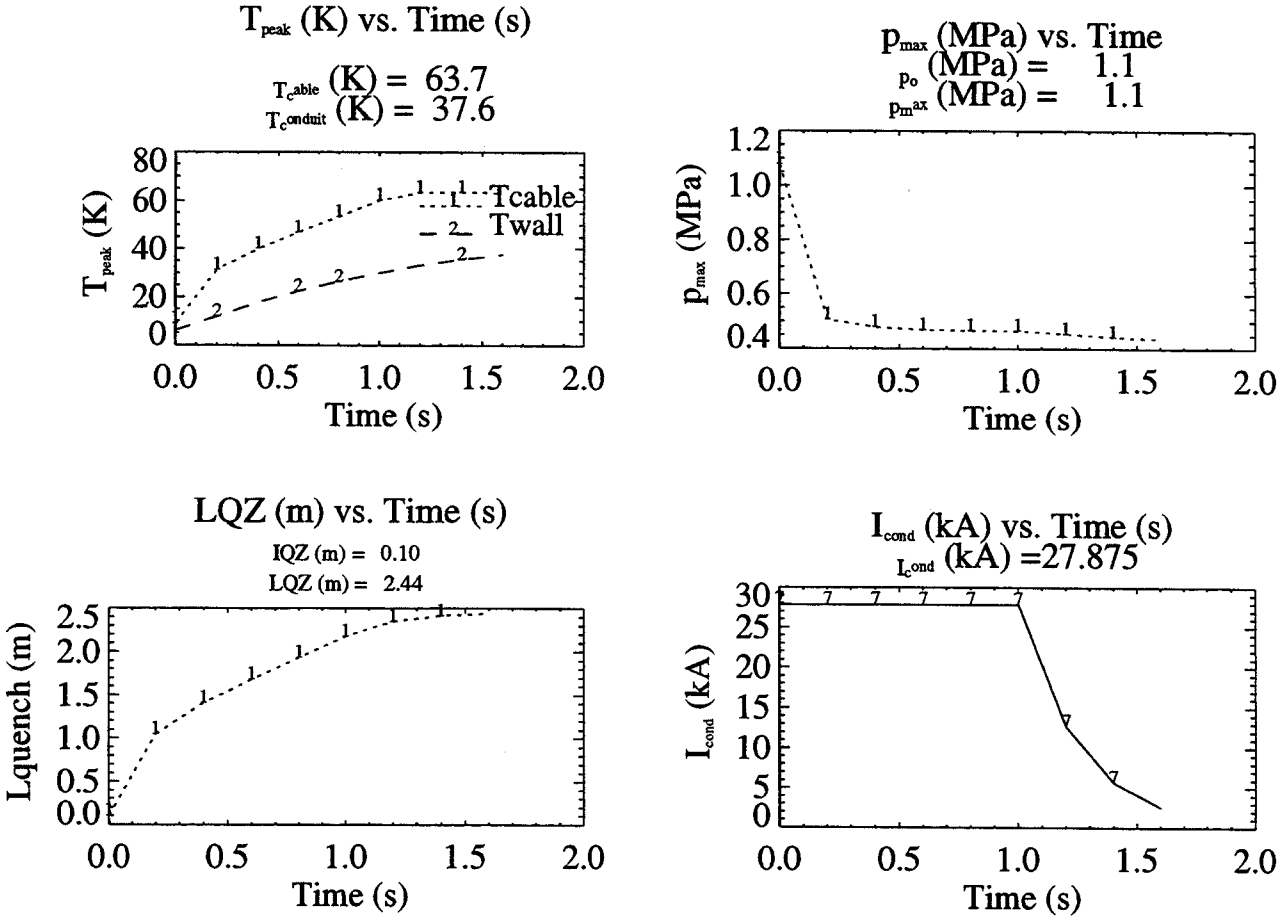

Figure 13: Peak temperature, pressure, quench length and current for an 0.1 m IQZ

As we have always observed, the peak temperature is highest for the lowest IQZ. This is because the helium rarefaction is stronger and occurs faster for a constant mass quench. The peak cable temperature of 63.7 K, while slightly higher than 57.1 K for a long quench is still far below the allowable of 150 K. Although the temperature of the conduit is still rising at 1.6 s, the temperature of the conductor is falling, so the conduit temperature won't go above 60 K. The calculation didn't take into account the sensors or the foil and took the most conservative interpretation of the area reduction by the twist pitch. Here the maximum

[14]14-940721-MIT/JSchultz-01, J.H. Schultz, "Quench/Dump Simulations of ECT PF Magnet," July 21, 1994

pressure is a nearly instantaneous spike to 1.1 MPa, relaxing rapidly to values not much larger than the original 4 atmospheres. The LQZ grows only to 2.44 m in 1.6 s. At the end of 1 s, the peak cable temperature is 60 K and the LQZ is 2.1 m. If we assume a linear temperature distribution down to 5 K at the quench propagation front, the approximate temperature length integral after 1 s is 68.3 m-K. Dividing the quench zone into five parts and applying the sensitivities listed above, this would give 611 fringe shifts. If there is a sharp temperature gradient near the quench propagating front, as there is in the TF simulation and in all other converging simulations we have observed, the number of fringe shifts will be even larger, perhaps equal to those in the TF system.

III.C Compliance with Design Criteria

Low IQZ quenches in the TF and PF magnets cause a minimum of 600 fringe shifts within a second. Neither a normal scenario nor a disruption cause more than 11 fringe shifts within a second in an entire winding pack. Simple signal-processing techniques, such as central difference averaging, should be able to reduce the number of fringe shifts from initiation or disruption over a second to less than one (obviously, there will be occasional individual fringe shifts from drift or other causes, so this becomes an irreducible minimum, if simple counters are used). A one second delay with a short IQZ was shown to cause peak temperatures in the TF of no higher than 65 K and in the TF of 146 K[15]. Since the quench will be detected in well under a second, the design criteria will be met.

IV: Cancellation of magnetic field

Magnetic field causes polarized light to rotate and fiber optic sensors can be used as magnetic field sensors. Two experiments were done at M.I.T. to verify the insensitivity of Mach-Zender and Michelson interferometers to D.C. and pulsed magnetic fields[16]. In these experiments, 10 meters of sense arm fiber were co-wound with a length of superconducting switch wire, and a length of stainless steel heater wire and all three were covered with a Teflon wrap. In addition, several turns of the reference fiber were wrapped around a piezoelectric transducer (PZT), which was used to modulate the length of the fiber, and another section of the reference fiber was held in a fiber polarization controller, which was used to match the polarizations in the two arms of the interferometer.

In order to determine if a change in fringe count was due to heating or cooling, the direction of the fringe movement was determined by sinusoidally modulating the reference arm, using the PZT, and demodulating the output of the detector with a phase sensitive detector, to generate a signal proportional to the derivative of the fringe with respect to length. This derivative was then used to determine the direction of motion of the fringe and either increase or decrease the fringe count appropriately. Figure 14 shows a schematic diagram of the prototype fiberoptic sensor.[17]

---

[15]13-940302-MIT-ASHAJII-01, A. Shajii, "Analysis of quench in the TPX TF coil ," March 2, 1995

[16] TPX No:1314-941130-MIT/SSmith-01, S. Smith and S. Ezekiel, "Improved Fiberoptic Quench Detection at the Francis Bitter National Magnet Laboratory, Rev. 1," Nov 30, 1994

[17]S. P. Smith and S. Ezekiel, "Optical Fiber Thermometry at Liquid Nitrogen Temperatures", ITER/US/94/EV-MAG/S.Smith/6.21/-1, June 21, 1994 and S.P. Smith and S. Ezekiel, "Fiberoptic Quench Detector: Liquid Helium Tests", ITER/US/94-EV-MAG/S. Smith/7.20/1, TPX 1314-94-0720-MIT-SSmith-01, July, 19, 1994,

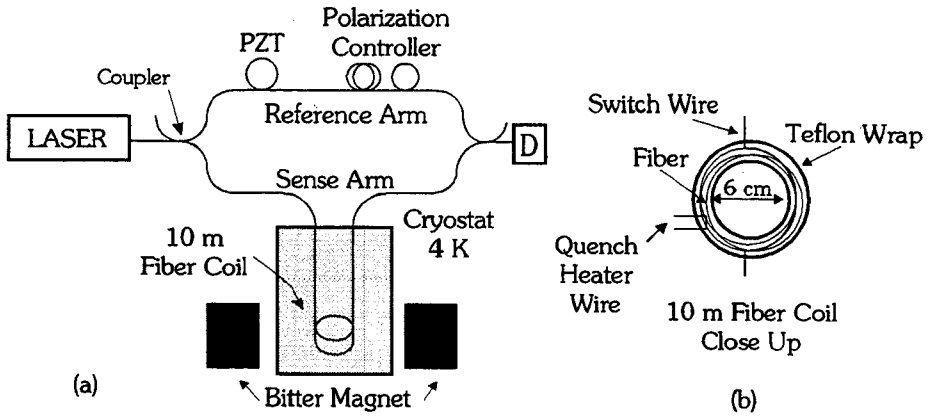

Figure 14 Schematic diagram of prototype fiberoptic quench detector (a) and closeup of fiber coil (b).

The sensitivity of phase to field was miniscule, while the sensitivity to the field ramp rate was low. If we attribute all drift to magnetic field changes, which is implausibly conservative, the field sensitivity is still no higher than 1 fringe /m-T. Similarly, if we attribute all noise in the instrumentation to the fiber optic and none to the rest of the data acquisition system, the maximum dB/dt sensitivity is 0.2 fringe/(m-T/s). It is probable that almost all of the ramp-rate signal is due to voltage pickup in some part of the apparatus, other than the fiber optic sensor. The measured fringe signals are shown in Figs. 15 and 16.

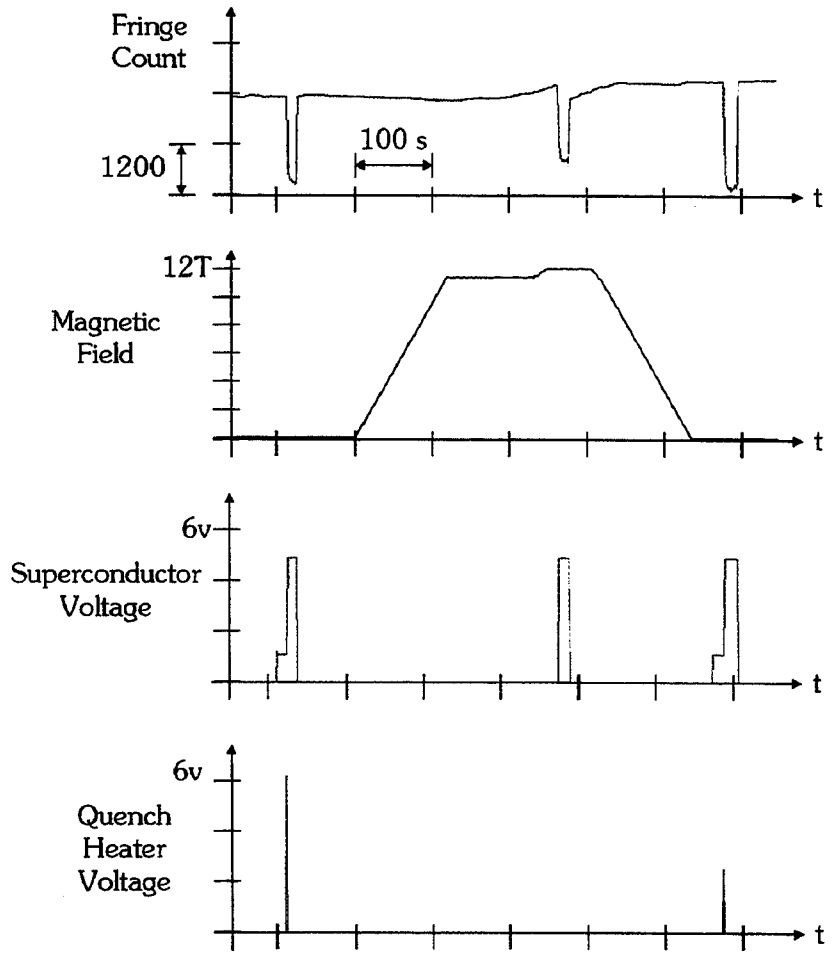

Figure 15 Quenches before, during and after a background field sweep

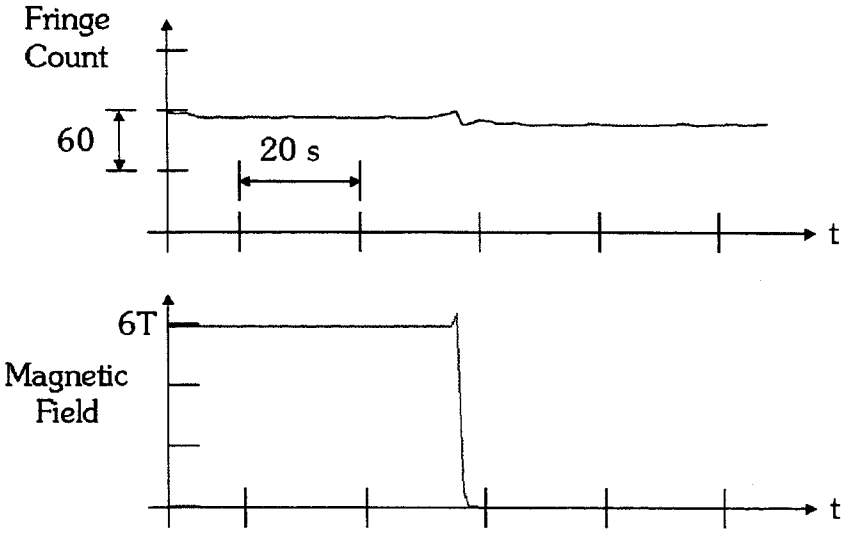

Figure 16 Insensitivity of the fiberoptic sensor to high rate of change in the background magnetic field

V: Cancellation of mechanical strain

The basic principle of fiber optic temperature sensing is that the index of refraction of glass is temperature sensitive. The phase shift of light wave travelling through a linear medium of length L and index of refraction n is:

$$\Delta\varphi = \frac{2\pi nL}{\lambda} \tag{1}$$

Fiber-optic temperature sensors work by detecting changes in the optical path length. A change in optical path length can occur by the desired effect, the temperature sensitivity of the index of refraction, or by undesired changes in the mechanical strain in the glass. The change in phase from either effect is:

$$\Delta\varphi = \frac{2\pi}{\lambda}\left[n\Delta L + \Delta nL\right] \tag{2}$$

The fiber optic sensor also has a phase shift due to the thermal expansion of the glass fiber. The thermal expansion of fused silica at 4 K is $5 \times 10^{-7}\ K^{-1}$, according to Lebesque[18]. The problem is that the sensitivity of the fiber to mechanical strain appears, at first, to be much higher than that to temperature. For example, the strain in the superconductor is believed to be on the order of 4×10^{-3} due to cooldown, with relief due to Lorentz hoop forces of about 1×10^{-3}. According to Smith[19], a sensitivity of fiberglass to temperature on the order of 1 fringe/m-K, corresponds to a change in the index of refraction of 0.675×10^{-6}. Therefore, imagine that during an initiation blip, the Lorentz strain is relieved by 20 % from 0.1 % strain to 0.08 %. At the same time, the temperature of the helium rises by 1 K. If we want an accurate reading of the temperature rise, there has to be about a factor of 1,000 rejection of the mechanical strain.

One method of reducing the mechanical strain is simply to let the fiber be loose within its can. That this can be achieved was demonstrated by mechanical bending test about a 10 cm drum, reported above. In order to guarantee that mechanical strain is reject, a number of electronic signal-processing methods have also been suggested. Investigators at ADVEC proposed using high-pass filtering for thermal excursions. This is unlikely to work, because the noisy tokamak environment doesn't favor high-pass filters and because the time signature of a quench and noise disturbances, such as initiation or disruptions is not different by orders of magnitude. A second method has been proposed and tested by Tsukumoto at the University of Yokahama[20]. This method involves the use of a dual-core optical fiber, where each core has a different index of refraction. The equation for the phase shift due to temperature or strain would then be:

---

18. H.J.M. Lebesque, B.S. Blaisse and E.F. Scheele, "Thermal expansion coefficient, refractive index and double refraction of crystalline quartz between 4 and 270 K," in *Problems of Low Temperature Physics and Thermodynamics*, Vol.2, Proc. of the International Institute of Refrigeration Commission I, Eindhoven, 1960, Ed. by A. Van Itterbeek, Pergamon Press, New York, 1962

[19] ITER/US/94-EV-MAG/S.Smith/7.20/1, Stephen Smith and S. Ezekiel, "Fiberoptic Quench Detector: Liquid Helium Tests," July 20, 1994

[20] O. Tsukamoto, K. Kawai, and Y. Kokubun, "Quench detection of superconducting magnet by dual-core optical fiber," IEEE Trans Mag, Vol. MAG-23, No. 2, March 1987

$$\frac{\Delta\Phi}{L\Delta T} = \frac{2\pi}{\lambda_0}\left\{\left(\frac{n_1 - n_2}{L}\frac{dL}{dT}\right) + \left(\frac{dn_1}{dT} - \frac{dn_2}{dT}\right)\right\} \quad (3)$$

where $\Delta\Phi$ is the change in the phase difference between the the two cores (radians), n_1 and n_2 are the refractive indices of the two cores, ΔT is the temperature change of the fiber (K), and λo is the wavelength of the laser light (m). A temperature sensor of this sort was tested along with a superconducting winding at Yokahama and appeared to "work." However, inspection of the paper along with elementary theoretical considerations indicate that the signal must inevitably be reduced in the same proportion as the noise, due to the cross-coupling terms. Given that the use of two cores in a one core is a serious constraint on fabricability, survivability, and cost, the dual-core technique also appears to be unworkable for TPX.

A method suggested by Ezekiel and Smith appears to be extremely promising over a broad range of strains and temperatures and has also been confirmed by experiment. In this method, two signals are sent through a fiber with different strain and temperature dependences. The simplest method is if the two dependences are very close in their strain dependence, but very different in their temperature dependence. Then the signals can be interfered at the end, and the strain effect would be largely canceled. The strain signal from one of them is multiplied and subtracted from that of the other in order to eliminate the strain effect (just like reducing a matrix in linear algebra). This can be done by sending two light signals down a single fiber that have any one of three differentiating properties: 1) Two colors, 2) Two modes, or 3) two polarities. The latter requires a polarization maintaining (PM) fiber. The differential strain and temperature sensitivities of this differential technique were measured by Vengsarkar[21] and are shown in Table III.

Table III: Sensitivity of Dual-Mode and Dual-Polarity Fiber to Temperature and Strain

Method	Temperature sensitivity	Strain sensitivity
	(radians/m-K)	(radians/m-ε) (radians/m-(dl/l))
2 Polarities	1.2	5×10^3
2 Modes	2.18	55×10^3

Without using either dual polarity or dual mode signal, a Mach-Zender interferometer would have a strain sensitivity at 800 nm of 7,850,000 radians/(m-ε). Thus, the dual polarization interferometer reduced the strain sensitivity by a factor of 1,570; while the dual mode interferometer reduced the strain sensitivity by a factor of 143.

By using both methods at once, theoretically perfect cancellation of mechanical strain could be achieved or a perfect cancellation of the temperature sensitivity. This technique was

[21] A.M. Vengsarkar, W.C. Michie, L. Jankovic, B. Culshaw, and R.O. Claus, "Fiberoptic sensor for simultaneous measurement of strain and temperature," Proc of the SPIE, Vol 1367, Fiber Optics and Laser Sources VIII (1990)

shown to work with polarization maintaining opitcal fiber in an experiment that duplicated Tsukamoto's dual-core fiber apparatus[22]. A description of the experiment is repeated here.

V.A Experimental Results

For this test a bundle of several optical fibers covered with an s-glass braid was epoxied to the outside of a small Nb-Ti layer wound magnet (4 layers, 20 turns/layer, 4 inch diameter). A strain gauge and thermocouple were also attached to the magnet, and the magnet was covered with a thin layer of styrofoam. In order to produce an adjustable strain on the optical fibers, the superconducting magnet was placed in a 7 Tesla background magnetic field produced by the 10A Bitter magnet at the Francis Bitter National Magnet Laboratory. Thus, by adjusting the current in the superconducting magnet, the strain applied to the fibers could be adjusted.

Figure 17 shows the result of this applied strain on a fiberoptic Michelson interferometer, as would be used for an internally terminated fiberoptic in a CICC, and a polarimetric interferometer. The upper left panel in the figure shows the current in the superconducting magnet which was ramped to 800 Amps (no background field in this case) with the horizontal scale marked in 1/5th of a second intervals. The upper right panel shows the output of the conventional strain gauge which closely follows the current in the superconducting magnet and shows a peak strain of about 0.01%. The lower right panel shows the output of the conventional fiberoptic Michelson interferometer in which the sense arm of the interferometer is wrapped around the magnet, and the reference arm unperturbed. As seen in the figure, the output of this interferometer closely tracks the strain gauge output. Finally, the output of the polarimetric interferometer is shown in the lower left panel, where the sense and reference arm of the interferometer are orthogonal polarizations in the same length of polarization maintaining fiber which is wrapped on the magnet, shows no response to the applied strain.

Figure 18 shows response of the polarimetric sensor as the current in the superconducting magnet is ramped until the magnet quenches. Starting at the upper left panel and moving clockwise the figure shows the current in the superconducting magnet which quenched at about 450 Amps, the strain, which had a peak of about 0.1%, the output of the thermocouple, and the fringe count from the polarimetric sensor. As seen in the figure, though 0.1% strain was applied to the fiber, only one fringe of movement is observed in the output of the interferometer as the strain was applied. In contrast, after the superconducting magnet quenched, at about the 100 point mark in the figure, a sharp rise in the fringe count and the thermocouple voltage is observed due to the heating of the magnet.

[22]TPX No:1314-950424-MIT-SSmith-01, S. Smith, "Report on Fiberoptic Strain Sensitivity Reduction Experiments at the Francis Bitter National Magnet Laboratory on 3/16/1995," April 24, 1995

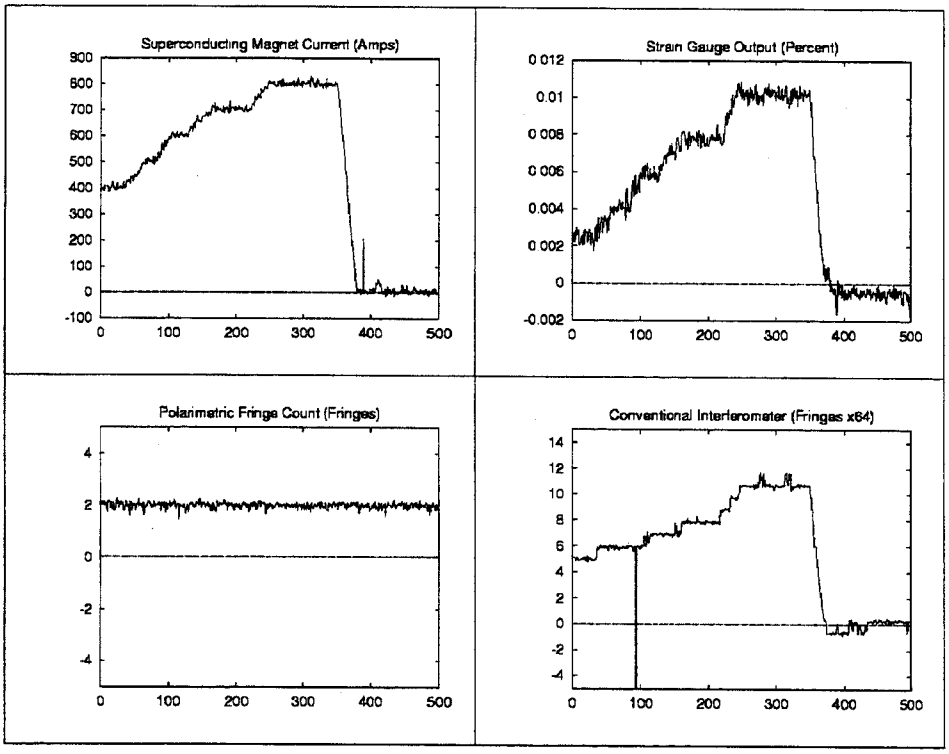

Figure 17 Example of strain applied to both Michelson and polarimetric interferometer.

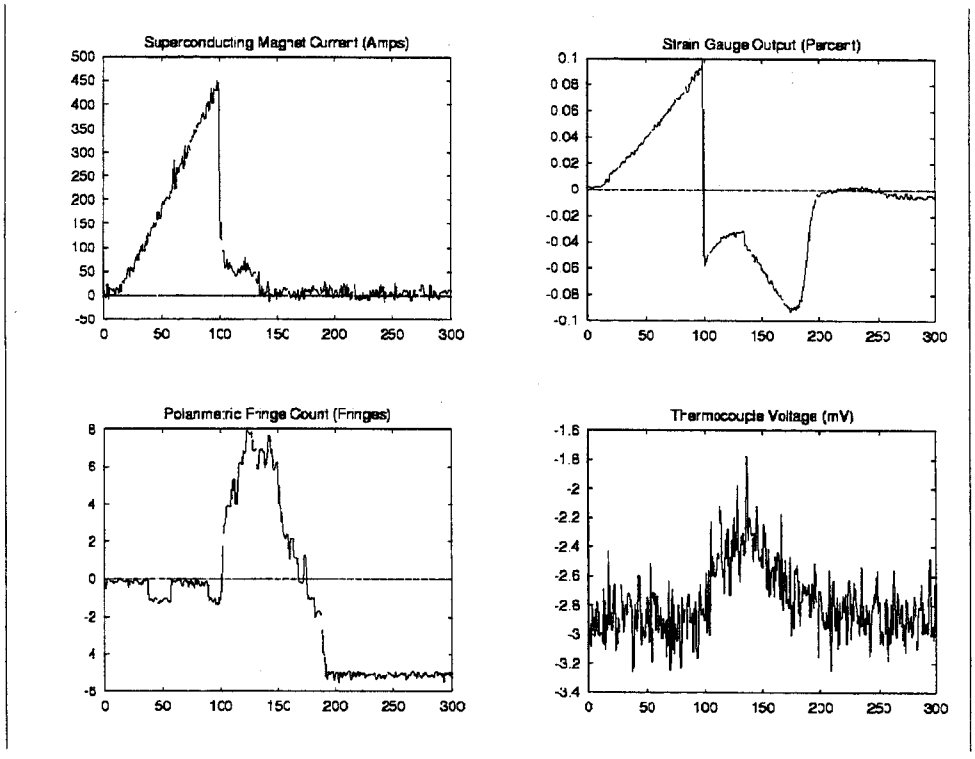

Figure 18 Superconducting magnet current sweep and quench.

VI. Cost

The quench detection sensors should not add significantly to the cost of a superconducting cable. It has been objected against fiber optic temperature sensors that they are too expensive. While it is true that fiber optic sensors are more expensive than S-glass insulated voltage sensors, a combination of redundancy and of cost-splitting between internal fibers, lasers, and signal-processing can be selected that achieves a high level of signal-noise along with a reasonable cost.

The cost of the system selected for the TPX design has been estimated as follows by Smith[23]: Due to the specialty nature of these specially coated fiberoptics, the cost for these fibers is much higher than the cost of commercial fiberoptics. Even in large quantities the cost of these fiberoptics is expected to be over $1/m, depending on the specific fiberoptic used.

Table IV: Internal Fiber Optic Temperature Sensor Cost

Component	Unit Cost	Redundancy x Length	Cost (k$)
Fiberoptic	$3/m	2x69km	$414k
Capillary tube, braid	$1.10/meter	69km	$76K
Total			$490k

Table V: FO Temperature Sensor Instrumenmation Costs

Item	Required for each	Cost	Number	Total
Lasers	8 fibers	$4k	15	$60k
Integrated Optics Chips	4 fibers	$4k	30	$120k
Detector-Counters	fiber	$500	120	$60k
Data Acquisition		$10k	2	$20k
Total				$260k

The total hardware cost of the fiber optic temperature sensing system is $750 k.

VII. Conclusions

Something is known about every aspect of the feasibility of reliable quench detection using internally wound fiber optic temperature sensors.

---

[23] TPX No: 1314-950628-MIT-SSmith-01, Stephen P. Smith, "Preliminary Quench Detection System Design Parts Count and Cost," June 28, 19995

Satisfaction of the TPX design criteria for signal-noise is demonstrated by simulation. Fringe-shift sensitivity to temperature changes is derived from direct measurements at liquid helium temperature. Signal-noise ratios of > 100:1 should be achievable within a second of quench propagation.

The ability of an optical fiber to survive encapsulation, cabling, conduit compaction, heat treatment, winding and extraction has been demonstrated by the copper-coated fiber in the QUELL coil.

The ability to extract an optical fiber, while maintaining a vacuum-tight seal against 70 atmospheres and two cooldowns to liquid helium temperature has been demonstrated[24].

The ability to reject false temperature signals due to mechanical strain has been demonstrated, using polarization-maintaining fiber.

---

[24] cf TPX No:1314-950709-MIT-JSchultz-01, J.H. Schultz et al, "Feasibility of the TPX voltage sensor quench detection system," July 9, 1995